Inorganic Chemistry

Article

pubs.acs.org/IC

Vapor-Controlled Linkage Isomerization of a Vapochromic Bis(thiocyanato)platinum(II) Complex: New External Stimuli To Control Isomerization Behavior

Atsushi Kobayashi,* Yuki Fukuzawa, Ho-Chol Chang, and Masako Kato*

Division of Chemistry, Faculty of Science, Hokkaido University, North-10 West-8, Kita-ku, Sapporo 060-0810, Japan

Supporting Information

ABSTRACT: We synthesized a novel Pt(II)−diimine complex with a typical ambidentate thiocyanato ligand, [Pt(*thiocyanato*)$_2$(H_2dcbpy)] (**1**; H_2dcbpy =4,4′-dicarboxy-2,2′-bipyridine), and found that the complex **1** exhibits unique linkage isomerizations with drastic color and luminescence changes driven by exposure to volatile organic chemical (VOC) vapors in the solid state. Reaction between [$PtCl_2$(H_2dcbpy)] and KSCN in aqueous solution at 0 °C enabled successful isolation of an isomer with the S-coordinated thiocyanato ligand, [Pt(SCN)$_2$(H_2dcbpy)] (**1SS·H_2O**), as a nonluminescent orange solid. Interestingly, **1SS·H_2O** was isomerized completely to one isomer with the N-coordinated isothiocyanato ligand, [Pt(NCS)$_2$(H_2dcbpy)] (**1NN·3DMF**) by exposure to DMF vapor, and this isomerization was accompanied by significant color and luminescence changes from nonluminescent orange to luminescent red. IR spectroscopy and thermogravimetric analysis revealed that adsorption of the DMF vapor and transformation of the hydrogen-bonded structure both played important roles in this vapor-induced linkage isomerization. Another isomer containing both S- and N-coordinated thiocyanato ligands, [Pt(SCN)(NCS)(H_2dcbpy)] (**1SN**), was obtained as a nonluminescent yellow solid simply by exposure of **1SS·H_2O** to acetone vapor at room temperature, and about 80% of **1SS·H_2O** was found to be converted to **1SN**. In the solution state, each isomer changed gradually to an isomeric mixture, but pure **1SS** was regenerated by UV light irradiation ($\lambda_{irr.}$ = 300 nm) of an MeOH solution of the mixture. In the crystal structure of **1SN**, the complex molecules were hydrogen-bonded to each other through the carboxyl groups of the H_2dcbpy ligand and the N site of the thiocyanato ligand, whereas the **1NN** molecules in the **1NN·4DMF** crystal were hydrogen-bonded to the solvated DMF molecules. Competition of the hydrogen-bonding ability among the carboxyl groups of the H_2dcbpy ligand, N and S atoms of the thiocyanato ligand, and the vapor molecule was found to be one of the most important factors controlling linkage isomerization behavior in the solid state. This unique linkage isomerization controlled by vapor can provide an outstanding vapochromic system as well as a new molecular switching function driven by vapor molecules.

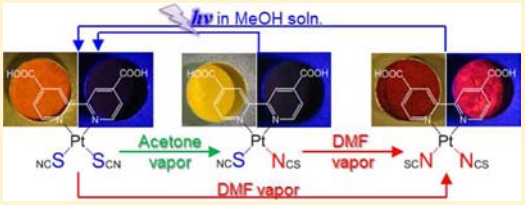

INTRODUCTION

The design and synthesis of stable and reversible chemical sensors have drawn considerable attention in the past decade.[1] Materials showing some chromotropic behaviors play a critical role in the function of such chemical sensing devices. For example, vapochromic materials showing reversible color changes in response to volatile organic compounds (VOC) are promising for construction of a chemical sensing device.[2−17] Although many vapochromic materials have been reported to date, these materials can be classified into three types of compounds on the basis of the origin of their vapochromism (Scheme 1). One type comprises materials that use intermolecular metallophilic and/or π−π stacking interactions (*Type-I*).[2−10] Most of these types of materials are primarily composed of either metal ions, such as Pt(II),[2−7] Au(I) and Ag(I) ions,[8] or organic molecules[9] with widely delocalized π electrons. This is because their d or π electronic orbitals enable them to overlap between molecules. The second type consists of materials that use a change in the coordination environment of the central metal ion or a change in the geometry of chromophoric ligand (*Type-II*).[11−15] Some Co(II),[11] Ni(II),[12] Cu(II),[13] and Au(I)[14] complexes are known to exhibit interesting vapochromic behaviors derived from the coordination and dissociation of the vapor molecules to/from the metal center. The third type is composed of materials with vapor-accessible channels[16] or dye-doped polymeric materials[17] that use host−guest interactions (*Type-III*). Some of the *Type-III* materials show only a slight color change in the ground state, but interesting luminescence changes are observed. These luminescence changes are primarily the result of exciplex formation between the host-framework and the adsorbed guest molecule or the solvent effect induced by the adsorbed guest molecules. Among these three types of vapochromic materials, Pt(II)-diimine-based molecules are one of the most promising and useful chromophores and luminophores. This is because both the color and luminescence of materials built from the Pt(II)-diimine chromophores are highly dependent on the interatomic distance of the Pt(II) ions. Many vapochromic Pt(II)−diimine complexes that take advantage of this distance-

Received: December 20, 2011
Published: June 26, 2012

   dx.doi.org/10.1021/ic202734f | *Inorg. Chem.* 2012, 51, 7508−7519

Scheme 1. Origins of Three Types of Vapochromic Systems

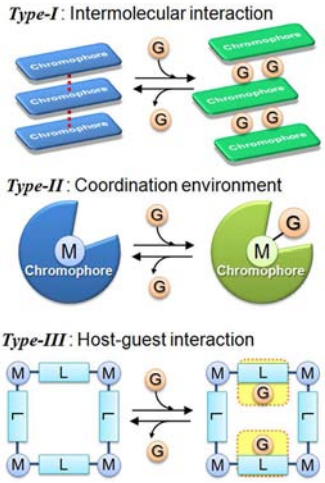

dependent chromophore have been reported to date.[2−7] However, to the best of our knowledge, there are few examples showing a change of molecular shape and/or coordination environment around the Pt(II) ion.[15a] If one can change the coordination environment of the Pt(II) ion in a vapochromic system using both *Type-I* and *Type-II* mechanisms, more drastic color and luminescence changes would be expected.

Photoinduced isomerizations accompanied by large changes in molecular shape are widely used to control physical properties and develop switching functions such as the photoinduced *cis*−*trans* isomerization of azobenzene[18] and photocyclization of diarylethene derivatives.[19] These isomerization reactions provide rich photochemistry and interesting switching functions on the basis of the photochromic properties of the compounds involved. For example, Nishihara et al. studied several types of azobenzene-functionalized transition metal complexes and achieved photo- and redox-controlled tristability.[20] Most isomerization reactions are controlled by light, temperature, and redox reactions, but there are no examples of their being controlled by exposure to VOC vapors as an external stimulus.

This study was conducted to develop a new type of vapochromic system that uses both the isomerization reaction and intermolecular metallophilic interaction of Pt(II) ions. We recently focused on the linkage isomerization behavior of the thiocyanato ligand (SCN^-), which is a typical ambidentate ligand that can coordinate to metal ions at both the S and N atoms to give different linkage isomers.[21−24] In our previous study, we reported that the linkage isomerization reaction of a Pt(II)−diimine complex with the thiocyanato ligand, [Pt(*thiocyanato*)$_2$(bpy)] (bpy = 2,2′-bipyridine), can be controlled by light irradiation and solution temperature among the three linkage isomers [Pt(SCN)$_2$(bpy)], [Pt(SCN)(NCS)(bpy)], and [Pt(NCS)$_2$(bpy)].[23c] However, this complex did not show any vapochromic behavior, and the two S-coordinated isomers, [Pt(SCN)$_2$(bpy)] and [Pt(SCN)(NCS)(bpy)], were thermally less stable than the N-coordinated isomer [Pt(NCS)$_2$(bpy)]. To achieve both vapochromic behavior and tristability on the basis of the three linkage isomers, we have designed a Pt(II)−diimine complex containing a proton-donating carboxyl group, [Pt(*thiocyanato*)$_2$(H$_2$dcbpy)] (**1**; H$_2$dcbpy =4,4′-dicarboxy-2,2′-bipyridine). This was done because it is well known that proton-donating groups tend to form hydrogen bonds with the proton-accepting N-site of the thiocyanato ligand, which would stabilize isomers having the S-coordinated thiocyanato ligand.[21] Here, we report the synthesis, structures, and linkage isomerization behavior of **1** among the three possible linkage isomers, [Pt(SCN)$_2$(H$_2$dcbpy)] (**1SS**), [Pt(SCN)(NCS)(H$_2$dcbpy)] (**1SN**), and [Pt(NCS)$_2$(H$_2$dcbpy)] (**1NN**). We also demonstrate that the linkage isomerization of **1** with drastic color and luminescence changes can be controlled by light irradiation and temperature, as well as by exposure of the solid sample to several VOC vapors. To the best of our knowledge, complex **1** is a novel type of vapochromic complex, which uses both changes in the intermolecular interaction (*Type-I*) and linkage isomerization of the molecule. This is the first example showing linkage isomerization induced by VOC vapors.

EXPERIMENTAL SECTION

General Procedures. All commercially available starting materials were used as received, and solvents were used without any purification. Unless otherwise stated, all manipulations were conducted in air. The starting complex, [PtCl$_2$(H$_2$dcbpy)], was prepared according to previously published methods.[25] The ^{1}H NMR spectrum of each sample was measured using a JEOL EX-270 NMR spectrometer at room temperature. Elemental analysis was conducted at the analysis center at Hokkaido University.

Synthesis of [Pt(SCN)$_2$(H$_2$dcbpy)] (1SS·H$_2$O). A solution of KSCN (194 mg, 2.0 mmol) in water (5 mL) was added to a solution of [PtCl$_2$(H$_2$dcbpy)] (51 mg, 0.10 mmol) in 0.03 M NaOH aqueous solution (13 mL) at 0 °C. After continuous stirring for 30 min, 2 M HNO$_3$ aqueous solution (2 mL) was added. The orange precipitates were then isolated by filtration, washed using 0.2 M HNO$_3$ aq., and dried under vacuum. Yield: 45 mg, 81% (based on [PtCl$_2$(H$_2$dcbpy)]. Elemental analysis calculated for C$_{14}$H$_8$N$_4$O$_4$PtS$_2$·H$_2$O: C 29.32, H 1.76, N 9.77. Found: C 29.51, H 2.01, N 9.63. ^{1}H NMR (0.01 M NaOD−D$_2$O, δ) for [Pt(SCN)$_2$(H$_2$dcbpy)]: 9.19 (d, 2H), 8.61 (s, 2H), 8.00 (d, 2H). IR (KBr, cm^{-1}): 3428 s, 3116 w, 3075 w, 2134 s, 1727 s, 1697 w, 1620 w, 1559 w, 1412 s, 1382 w, 1315 w, 1293 w, 1260 w, 1220 s, 1145 w, 1132 w, 1114 w, 1069 w, 935 w, 840 w, 825 w, 769 w, 751 w, 708 w, 665 m, 540 w.

Synthesis of [Pt(SCN)(NCS)(H$_2$dcbpy)] (1SN). Yellow crystals of **1SN** were obtained from recrystallization of **1SS** from acetone/H$_2$O (80/20 v/v). Elemental analysis calculated for C$_{14}$H$_8$N$_4$O$_4$PtS$_2$·H$_2$O: C 29.32, H 1.76, N 9.77. Found: C 29.78, H 1.61, N 9.58. IR (KBr, cm^{-1}): 3226 m, 3154 w, 3091 w, 3070 m, 2139 m, 2095 s, 1726 s, 1700 w, 1623 w, 1559 m, 1419 s, 1375 m, 1236 s, 1202 s, 1151 w, 1133 w, 1071 w, 940 w, 867 w, 820 w, 769 m, 747 w, 708 w, 682 w, 662 m, 540 w.

Synthesis of [Pt(NCS)$_2$(H$_2$dcbpy)]·*n*DMF (1NN·*n*DMF). Yellow crystals of **1NN·4DMF** were obtained by recrystallization of **1SS** from DMF. Red luminescent crystalline solid was obtained by exposure **1SS** to DMF vapor at room temperature for 1 day. Elemental analysis calculated for C$_{14}$H$_8$N$_4$O$_4$PtS$_2$·3DMF·H$_2$O: C 34.85, H 3.94, N 12.37. Found: C 34.94, H 3.70, N 12.27. IR (KBr, cm^{-1}): 3449 m, 3116 w, 3079 w, 2115 m, 2095 w, 1723 s, 1654 s, 1617 s, 1549 w, 1437 w, 1378 s, 1314 w, 1259 m, 1238 s, 1143 w, 1109 w, 1068 w, 932 w, 906 w, 862 w, 824 w, 767 m, 710 w, 682 w, 540 w.

Single-Crystal X-ray Diffraction Measurements. All single-crystal X-ray diffraction measurements were conducted using a Rigaku Mercury CCD diffractometer with graphite monochromated Mo Kα radiation (λ= 0.71069 Å) and a rotating anode generator. Each single crystal was mounted on a MicroMount using paraffin oil. The crystal was then cooled using an N$_2$-flow-type temperature controller. Diffraction data were collected and processed using the CrystalClear software.[26] Structures were solved by the direct method using SIR-2004.[27] Structural refinements were conducted by the full-matrix least-squares method using SHELXL-97.[28] Non-hydrogen atoms were refined anisotropically, hydrogen atoms bound to oxygen atoms were refined isotropically, and other hydrogen atoms were refined using the riding model. All calculations were conducted using the Crystal

dx.doi.org/10.1021/ic202734f | *Inorg. Chem.* 2012, 51, 7508−7519

Structure crystallographic software package.[29] Crystallographic data obtained for each complex are summarized in Table 1.

Table 1. Crystal Parameters and Refinement Data

complex	1NN·4DMF	1SN
T/K	150(1)	153(1)
formula	$C_{14}H_8N_4O_4PtS_2$·4DMF	$C_{14}H_8N_4O_4PtS_2$
formula weight	847.83	555.45
crystal system	triclinic	monoclinic
space group	P-1	$P2_1/c$
a/Å	6.893(3)	7.541(2)
b/Å	14.818(7)	9.180(3)
c/Å	16.875(9)	22.269(7)
α/deg	96.599(8)	90
β/deg	101.440(8)	98.7993(13)
γ/deg	94.349(8)	90
V/Å^3	1669.6(14)	1523.4(8)
Z	2	4
$D_{cal.}$/g cm^{-3}	1.686	2.422
Reflections collected	13106	11637
Unique reflections	7467	3463
GOF	1.091	1.151
R ($I > 2.00\sigma(I)$)	0.0670	0.0439
R_W[a]	0.1810	0.0882

[a] $R_W = [\Sigma(w(F_o^2 - F_c^2)^2)/\Sigma w(F_o^2)^2]^{1/2}$.

Powder X-ray Diffraction. Powder X-ray diffraction was conducted using a Rigaku SPD diffractometer at beamline BL-8B at the Photon Factory, KEK, Japan. The wavelength of the synchrotron X-rays was 1.200(1) Å. All samples were placed in a glass capillary with a diameter of 0.5 mmϕ.

UV–Vis Spectroscopy. The UV–vis absorption spectrum of each complex was recorded on a Shimadzu UV-2400PC spectrophotometer. The diffuse reflectance spectrum of each complex was recorded on the same spectrophotometer equipped using an integrating sphere apparatus. The obtained reflectance spectra were converted to absorption spectra using the Kubelka–Munk function $F(R_\infty)$.

Luminescence Properties. The luminescence spectrum of each sample was measured using a JASCO FR-6600 spectrofluorometer at room temperature. The slit widths of the excitation and emission light were 5 and 6 nm, respectively. The luminescence quantum efficiency was recorded on a HAMAMATSU C9920-02 absolute photoluminescence quantum yield measurement system equipped with an integrating sphere apparatus and 150 W CW xenon light source. The luminescence lifetime of each sample was recorded using a HAMAMATSU C4780 ps fluorescence lifetime measurement system equipped with a nitrogen laser light source (λ = 337.1 nm).

Thermogravimetric Analysis. Thermogravimetry and differential thermal analysis were conducted using a Rigaku ThermoEvo TG8120 analyzer.

IR Spectroscopy. For IR absorption measurements, samples were prepared by grinding powdered reagent with KBr, after which they were analyzed using a JASCO FT-IR 4100 spectrophotometer. Temperature-dependent IR spectra were measured using a Nicolet 6700 FT-IR spectrometer with a Nicolet Continuum microscope. The sample temperature was controlled by a Linkam LK-600 hot stage.

Linkage Isomerization Experiments. Photoirradiation experiments were conducted using a Perfect UV LAX-103 light source (Asahi Spectra Inc.) with optical filters (bandpass-type filters XBPA-300, XBPA-400, and XBPA-500).

RESULTS AND DISCUSSION

Synthesis and Thermal Stability of 1SS. As mentioned in the introduction, we previously reported the linkage isomerzation behavior of a nonsubstituted bipyridine–Pt(II) complex [Pt(*thiocyanato*)$_2$(bpy)] and found that it was important to regulate the temperature of the reaction solution during synthesis to control the isomeric ratio among the three possible isomers.[23c] A thermodynamically stable isomer with N-coordinated thiocyanate ligands, [Pt(NCS)$_2$(bpy)], can be obtained preferentially from the reaction solution at high temperature, whereas a kinetically favorable isomer [Pt(SCN)$_2$(bpy)] is obtained from the reaction at low temperature. Taking advantage of this feature, we synthesized [Pt(*thiocyanato*)$_2$(H$_2$dcbpy)] (**1**) at around 0 °C to isolate one isomer with S-coordinated thiocyanate ligands, [Pt(SCN)$_2$(H$_2$dcbpy)] (**1SS**). Figure 1(a) and (b) show the IR and ^{1}H NMR spectra of the orange solid obtained from the aqueous reaction solution at 0 °C. The IR band of the ν(C≡N) mode was observed at 2128 cm^{-1}, which is consistent with the band of the isomer of the nonsubstituted bipyridine complex with the S-coordinated thiocyanato ligand, [Pt(SCN)$_2$(bpy)] (2132 cm^{-1}).[23c] As shown in Figure 1(b), the ^{1}H NMR spectra produced in a 0.01 M NaOD–D$_2$O solution showed only three signals, i.e., one singlet and two doublets. In addition, the chemical shifts of these signals, especially the signal of α-proton of dcbpy ring (δ = 9.19, d, 2H), are very close to those of the isomer with S-coordinated thiocyanato ligand, [Pt(SCN)$_2$(bpy)] (δ = 9.37, d, 2H).[23c] These results indicate that the obtained orange solid is the pure isomer, [Pt(SCN)$_2$(H$_2$dcbpy)]. Elemental analysis indicated that the complex includes approximately equimolar amount of water molecules (**1SS·H$_2$O**). Because it is well known that the energy of the ν(C≡N) mode depends strongly on the coordination mode of the thiocyanate ligand,[21] the temperature dependence of the IR spectrum was measured to investigate the thermal stability of **1SS·H$_2$O** in the solid state. As shown in Figure 2, vibration bands attributable to the ν(C≡N) and ν(C=O) modes were observed around 2100 and 1700 cm^{-1}, respectively, but these changed significantly in response to rising temperature. Below 333 K, the observed spectra were almost identical to the spectra observed at room temperature, indicating that no isomerization occurred in this temperature

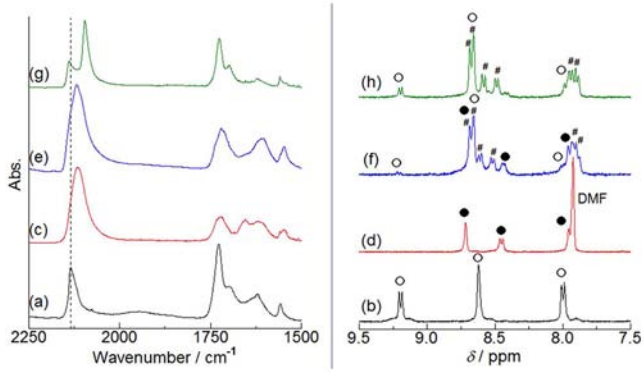

Figure 1. Solid-state IR and ^{1}H NMR spectra in D$_2$O–NaOD solution (aromatic region) of (a,b) as synthesized **1SS·H$_2$O**. (c,d) **1NN·3DMF** obtained from exposure of **1SS·H$_2$O** to DMF vapor for 1 d at room temperature. (e,f) Isomeric mixture obtained by heating **1NN·3DMF** at 150 °C for 6 h. (g,h) **1SN** obtained from exposure of **1SS·H$_2$O** to acetone vapor for 1 d at room temperature. The dotted line is a guide for the wavenumber of the ν(C≡N) mode in the SCN ligand. The symbols ○, ●, and, # indicate the signals for [Pt(SCN)$_2$(H$_2$dcbpy)], [Pt(NCS)$_2$(H$_2$dcbpy)], and [Pt(SCN)(NCS)(H$_2$dcbpy)], respectively.

dx.doi.org/10.1021/ic202734f | Inorg. Chem. 2012, 51, 7508–7519

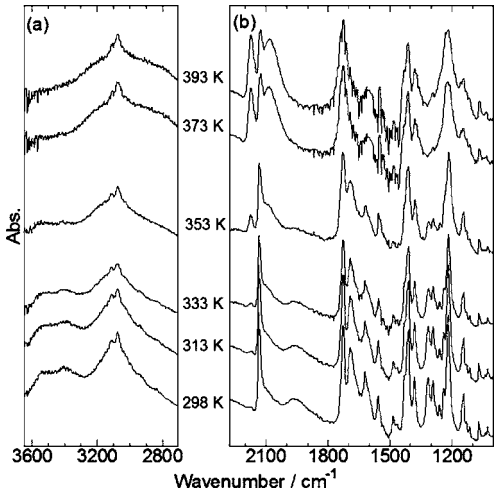

Figure 2. Temperature dependence of IR spectrum of **1SS·H_2O**. (a) Region of O−H and C−H stretching modes. (b) Region of C≡N, C═O, and C−O stretching modes.

region. The absorbance of the ν(O−H) mode of the hydrated water observed at around 3450 cm^{-1} was significantly lower at 353 K and almost completely gone above 373 K. In the same temperature region, the ν(C≡N) mode split into two sharp bands and one broad band. Consequently, some linkage isomerization reactions from **1SS** to the other isomers occurred above 353 K, and these were accompanied by the release of water molecules. In addition, the ν(C═O) mode observed around 1700 cm^{-1} as two split bands at 298 K was unified to one broad band and the absorbance of ν(C−O) mode at around 1300 cm^{-1} greatly decreased at temperatures above 373 K. These IR spectral changes suggest that the release of water molecules has a considerable effect on the crystal structure as well as the molecular structure; namely, it induces the linkage-isomerization reaction in the solid state.

Linkage Isomerization in the Solid State Induced by Vapors. Many Pt(II)−diimine complexes have been found to exhibit colorful vapochromic behavior on the basis of modification of the intermolecular metallophilic interaction induced by adsorption/desorption of vapor molecules.[2−7] Because the Pt(II) complex with the same diimine ligand, [$Pt(CN)_2(H_2$dcbpy)], shows colorful vapochromic behavior in response to various VOC vapors,[3c] the vapochromic response of **1SS·H_2O** was studied in detail.

1SS·H_2O showed interesting color changes in the presence of several VOC vapors. Figure 3 shows the changes of brightfield and luminescence images and UV−vis diffuse reflectance and luminescence spectra of **1SS·H_2O** in response to exposure to DMF and acetone vapor for 1 d. As shown in Figure 3(a), the color of **1SS·H_2O** changed significantly in response to exposure to these organic vapors from orange to dark red and yellow under DMF and acetone vapor, respectively. It should be noted that the nonluminescent **1SS·H_2O** was converted to a red luminescent solid upon exposure to DMF vapor. As shown in Figure 3(b) and (c), the absorption band around 500 nm was shifted to a wavelength that was about 80 nm longer, and a new luminescence band at 660 nm ($\Phi_{em.}$= 0.05) appeared in response to exposure of **1SS·H_2O** to DMF vapor, whereas the absorption band of **1SS·H_2O** was shifted to a wavelength that was approximately 20 nm shorter in response to exposure to acetone vapor. The absorption bands produced by the Pt(II)−diimine complex series in the visible region are usually assigned to either the metal-to-ligand charge-transfer (MLCT) transition or metal−metal-to-ligand charge-transfer (MMLCT) transition.[30,31] In the latter case, the effective metallophilic interaction between Pt(II) ions usually generates the emissive ^{3}MMLCT transition state, resulting in strong phosphorescence. Thus, the large red shift and appearance of the red emission at 660 nm for the dark red solid obtained by exposure of **1SS·H_2O** to DMF vapor suggest that a structural transformation occurs to generate more effective metallophilic interaction between Pt(II) ions. The observed emission energy and the lifetime of about 61 ns are comparable to the ^{3}MMLCT emission observed for the Pt(II)−diimine complex [Pt(bpy)$(CN)_2$] (bpy = 2,2′-bipyr-

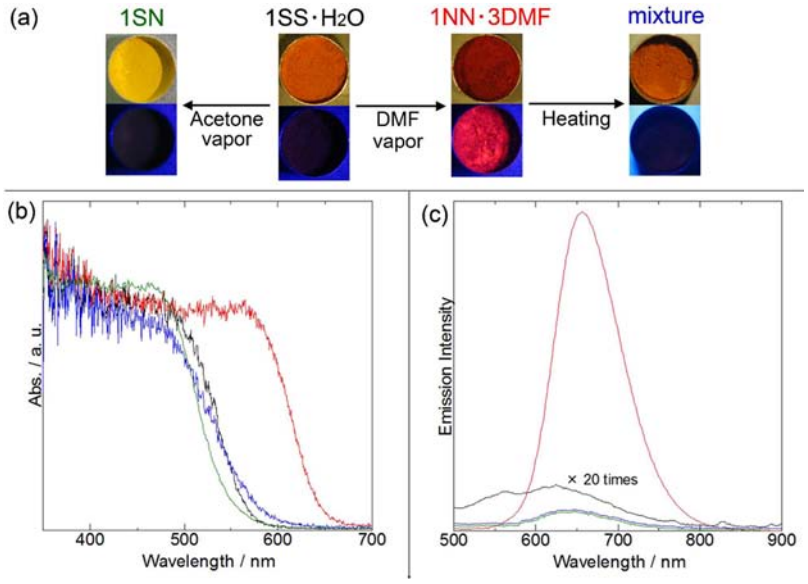

Figure 3. (a) Brightfield and luminescence images. (b) UV−vis diffuse reflectance. (c) Luminescence spectra of as synthesized **1SS·H_2O** (black), **1NN·3DMF** obtained from exposure of **1SS·H_2O** to DMF vapor for 1 d at room temperature (red), isomeric mixture obtained from heating **1NN·3DMF** at 150 °C for 3 h (blue), and **1SN** obtained from exposure of **1SS·H_2O** to acetone vapor for 1 d at room temperature (green).

dx.doi.org/10.1021/ic202734f | Inorg. Chem. 2012, 51, 7508−7519

idine) with the effective metallophilic interaction ($\lambda_{em.}$ = 600 nm, $\tau_{em.}$ = 160 ns).[30c,e] Conversely, the observed blue shift in UV−vis diffuse reflectance spectra in response to exposure of **1SS·H$_2$O** to acetone vapor implies that the structural transformation may involve a movement to reduce the intermolecular metallophilic and/or π−π stacking interaction.

To clarify the origin of these interesting color changes, the IR and ^{1}H NMR spectra for each sample were analyzed. As shown in Figure 1(c), the dark red solid obtained by exposing **1SS·H$_2$O** to DMF vapor produced a ν(C≡N) band at 2115 cm^{-1}, which was about 13 cm^{-1} lower than that produced by unexposed **1SS·H$_2$O**. Surprisingly, the proton signals observed in the ^{1}H NMR spectrum, as shown in Figure 1(d), were composed of two doublets and one singlet with chemical shifts that differed significantly from those produced by **1SS·H$_2$O**. These IR and ^{1}H NMR spectra indicate that the obtained red solid is composed of only one isomer with a symmetrical molecular structure, that is, the isomer with the N-coordinated isothiocyanato ligands, [Pt(NCS)$_2$(H$_2$dcbpy)] (**1NN**). Observed high-field shifts of three proton signals in **1NN** compared to the signals of **1SS** are due to both the weaker *trans* effect and the stronger π-back-donation of the N-coordinated isothiocyanato ligand than those of the S-coordinated thiocyanato ligand, resulting in the smaller population of the shielding π electron of dcbpy ligand in **1NN** than that in **1SS**. In addition, the ν(C═O) band at 1653 cm^{-1} and the proton signal at 7.92 ppm assignable to the DMF molecule were observed upon analysis of the IR and ^{1}H NMR spectra, respectively. Thermogravimetric and elemental analyses revealed that the red luminescent sample adsorbed approximately 3 mol mol^{-1} DMF and then released it in two steps when the temperature was raised to 150 °C (Figure S1 of the Supporting Information). Thus, these results clearly indicate that **1SS·H$_2$O** was completely converted to **1NN·3DMF** and that this was accompanied by the adsorption of DMF vapor. Considering that the ν(C═O) band of the DMF molecule was shifted to about 22 cm^{-1} lower than that of normal liquid DMF (1675 cm^{-1}), the adsorbed DMF molecules probably form hydrogen bonds with the carboxyl group of the H$_2$dcbpy ligand.

After removing the DMF by heating, the red luminescent **1NN·3DMF** was converted to a nonluminescent orange solid, as shown in Figure 3(a). The IR and ^{1}H NMR spectra of this DMF-removed orange solid are shown in Figure 1(e) and (f), respectively. The ν(C═O) band of the DMF molecule disappeared completely and the ν(C≡N) band at 2115 cm^{-1} was broadened after the removal of DMF vapor. In the ^{1}H NMR spectrum, proton signals assigned to **1SS** and **1NN** and six proton signals derived from the asymmetric bipyridine ring were observed, suggesting the existence of an isomer containing both thiocyanato and isothiocyanato ligands, **1SN**. The isomeric ratio of this DMF-removed sample was estimated to be **1SS**:**1SN**:**1NN** = 5:68:27 on the basis of the ^{1}H NMR spectrum, implying that the **1SN** may be more stable than **1NN** without vapor molecules. These IR and ^{1}H NMR spectral changes indicate that **1NN·3DMF** was converted to an isomeric mixture of three isomers by removal of DMF. It should be emphasized that this orange solid consisting of a mixture of three isomers was successfully converted back to the red luminescent **1NN·3DMF** completely by exposure to DMF vapor. In addition, complete linkage isomerization from **1SS** to **1NN** was never observed in DMF solution or other solutions (see below). Consequently, the adsorption of DMF vapor in the solid state plays a critical role in the complete linkage isomerization from **1SS** or three-isomer mixtures to **1NN**.

In contrast, the nonluminescent yellow solid obtained by exposing **1SS·H$_2$O** to acetone vapor showed significantly different IR and ^{1}H NMR spectra, as shown in Figure 1(g) and (h). The ν(C≡N) band of the thiocyanato ligand consisted of two widely split bands at 2139 and 2095 cm^{-1}. A low-wavenumber-shifted ν(C≡N) band is a well-known characteristic of the N-coordinated isothiocyanato ligand.[21] In the ^{1}H NMR spectrum, six proton signals assignable to the asymmetric bipyridine moiety were observed in addition to slight residual signals of **1SS**. Thus, **1SS·H$_2$O** is thought to be primarily converted to a linkage isomer with an asymmetric molecular structure, [Pt(SCN)(NCS)(H$_2$dcbpy)] (**1SN**). The integral ratio of the proton signals of **1SN** to those of **1SS** in the ^{1}H NMR spectrum suggests that about 80% of the **1SS** was converted to **1SN**. In addition, the observed powder X-ray diffraction pattern for this yellow solid was almost identical to the simulation calculated from the crystal structure of **1SN**, as discussed below (see Figure 4). In contrast to the linkage isomerization from **1SS·H$_2$O** to **1NN·3DMF** induced by DMF vapor, no vibration bands assignable to acetone vapor were observed in the IR spectra of **1SN**. On the basis of the fact that no water molecules were observed in the crystal structure of **1SN** and the synthesized **1SS·H$_2$O** contains crystal water at about 1 mol mol^{-1}, desorption of water molecules induced by exposure to acetone vapor may promote linkage isomerization from **1SS** to **1SN**. Indeed, thermogravimetric analysis of the yellow solid **1SN** up to 150 °C revealed only negligible weight loss (about 0.24%), suggesting that **1SN** does not contain any hydrated water molecules (Figure S2 of the Supporting Information). It should be emphasized that the yellow solid of **1SN** was never converted to the other isomers during thermal treatment at temperatures up to 150 °C in air (Figure S3 of the Supporting Information), but that it was completely

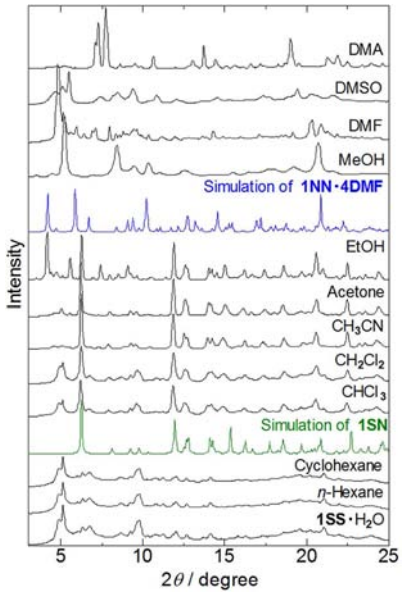

Figure 4. Changes in PXRD pattern of **1SS·H$_2$O** under exposure to various organic vapors for one week at room temperature. The two colored lines show simulation patterns calculated from the crystal structures of **1NN·4DMF** (blue) and **1SN** (green).

dx.doi.org/10.1021/ic202734f | Inorg. Chem. 2012, 51, 7508−7519

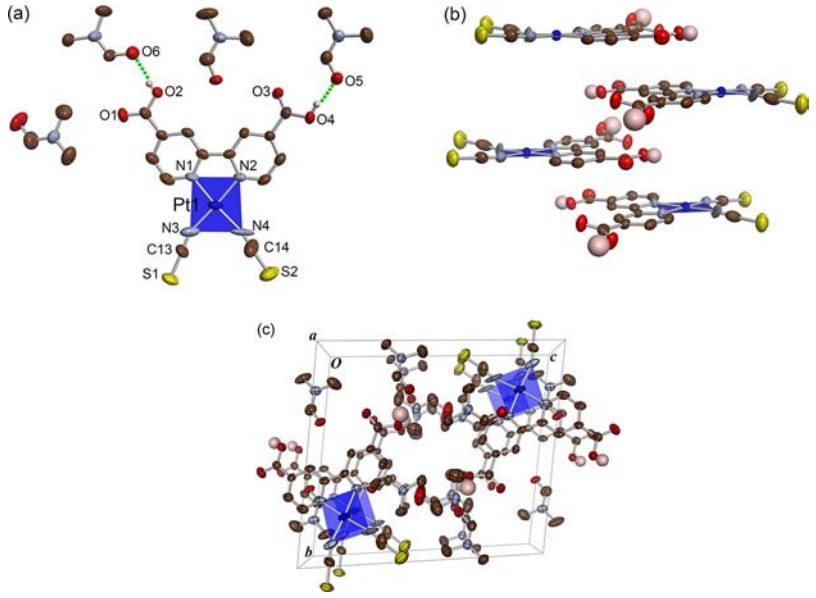

Figure 5. (a) Molecular structure in one asymmetric unit. (b) 1-D stacked structure, and (c) packing diagram viewed along the *a* axis of **1NN·4DMF**. H atoms bonded to C are omitted for clarity. DMF molecules are omitted for clarity in (b). The coordination sphere of the Pt(II) ion is shown in the blue plane. Brown, light blue, red, and yellow ellipsoids, and pink balls represent C, N, O, S, and H atoms, respectively. Green dotted lines in (a) show the hydrogen bonds between 1NN and DMF molecules.

converted to **1NN·3DMF** by exposure to DMF vapor for 1 d at room temperature (Figure S4 of the Supporting Information).

To clarify the vapor dependency of linkage isomerization in the solid state, PXRD measurements for several samples obtained by exposure of **1SS·H_2O** to various organic vapors for one week at room temperature were conducted. As shown in Figure 4, the PXRD pattern of **1SS·H_2O** changed remarkably in response to exposure to relatively highly polar organic vapors such as dimethyl sulfoxide (DMSO) and CH_3CN, whereas no change was observed in response to exposure to nonpolar organic vapors such as *n*-hexane. Surprisingly, the PXRD patterns observed in response to exposure to $CHCl_3$, CH_2Cl_2, CH_3CN, acetone, and EtOH vapors were almost identical to the simulated results calculated from the crystal structure of **1SN** (see below), except for the low-angle region, where minor diffraction peaks derived from unconverted **1SS·H_2O** were observed. The IR spectra of these samples also showed characteristic ν(C≡N) bands that were widely split into two bands at 2139 and 2095 cm^{-1} (Figure S5 of the Supporting Information). These changes indicate that most of the **1SS·H_2O** was converted to **1SN** in response to exposure to these moderately polar vapors. Additional diffraction peaks observed in the sample exposed to EtOH vapor (e.g., 4.1°, 5.6°, and 7.4°) suggests the existence of the other structural phases. In contrast, exposure of **1SS·H_2O** to highly polar MeOH, DMF, DMSO, and *N*,*N*-dimethylacetamide (DMA) vapors cause the pattern of **1SS·H_2O** to become completely different from the original pattern of **1SS·H_2O**, suggesting that the structural transformations were induced by these vapors and that these structures are strongly dependent on the vapor molecules. Disagreement between the simulation of **1NN·4DMF** (see below) and the PXRD pattern observed in response to exposure to DMF vapor may be derived from differences in adsorbed DMF molecules. The ^{1}H NMR spectra in a 0.01 M NaOD−D_2O solution of the samples exposed to DMSO and DMA vapor were identical to that of **1NN·3DMF** (Figure S6 of the Supporting Information). Consequently, **1SS** was completely converted to **1NN** by exposure to these highly polar aprotic organic vapors. In addition, these **1NN·*n*(vapor)** samples obtained by exposing **1SS** to DMA or DMSO vapor exhibit bright luminescence at 628 and 638 nm (Figure S7 of the Supporting Information), suggesting that the emission energy of **1NN** strongly depends on the adsorbed vapor molecule. On the other hand, ^{1}H NMR spectra in 0.01 M NaOD−D_2O solution of the samples exposed to MeOH and EtOH vapor suggest that these samples are mainly composed of the **1SN** isomer, but the other isomers are also included (Figure S6 of the Supporting Information). The isomeric ratios of MeOH- and EtOH-exposed samples are estimated to be **1SS**:**1SN**:**1NN** = 0:70:30 and 19:51:30, respectively. These results suggest that **1SS·H_2O** can isomerize in the solid state to the other linkage isomers **1SN** and **1NN** upon exposure to various organic solvent vapors. The linkage isomerization from **1SS** to **1NN** could be triggered by the adsorption of highly polar vapors, whereas the isomerization from **1SS** to **1SN** would proceed by exposure to moderately polar vapor but the adsorption of vapor would not be involved in this linkage isomerization.

Crystal Structures. As discussed above, vapor-induced linkage isomerization of complex **1** was primarily studied by solid-state IR and ^{1}H NMR spectra in solution because each linkage isomer exhibits characteristic features in both spectra. To make the structure of each linkage isomer clear, we have prepared two single crystals composed of **1NN** or **1SN**. In this section, we discuss the molecular and crystal structures of these crystals.

Figure 5(a) shows the obtained molecular structure of **1NN·4DMF**. Both thiocyanate ligands were found to be bound to the Pt(II) ion by the N atom. All atoms in the [Pt(NCS)$_2$(H_2dcbpy)] molecule are located on the same plane. The Pt1−N3 and Pt1−N4 distances (1.984(10) Å and 2.056(12) Å, respectively) were within the range of typical values for Pt−N coordination bonds.[32] The Pt1−N3−C13 and Pt1−N4−C14 angles were 158.0(9)° and 159.9(13)°,

dx.doi.org/10.1021/ic202734f | *Inorg. Chem.* 2012, 51, 7508−7519

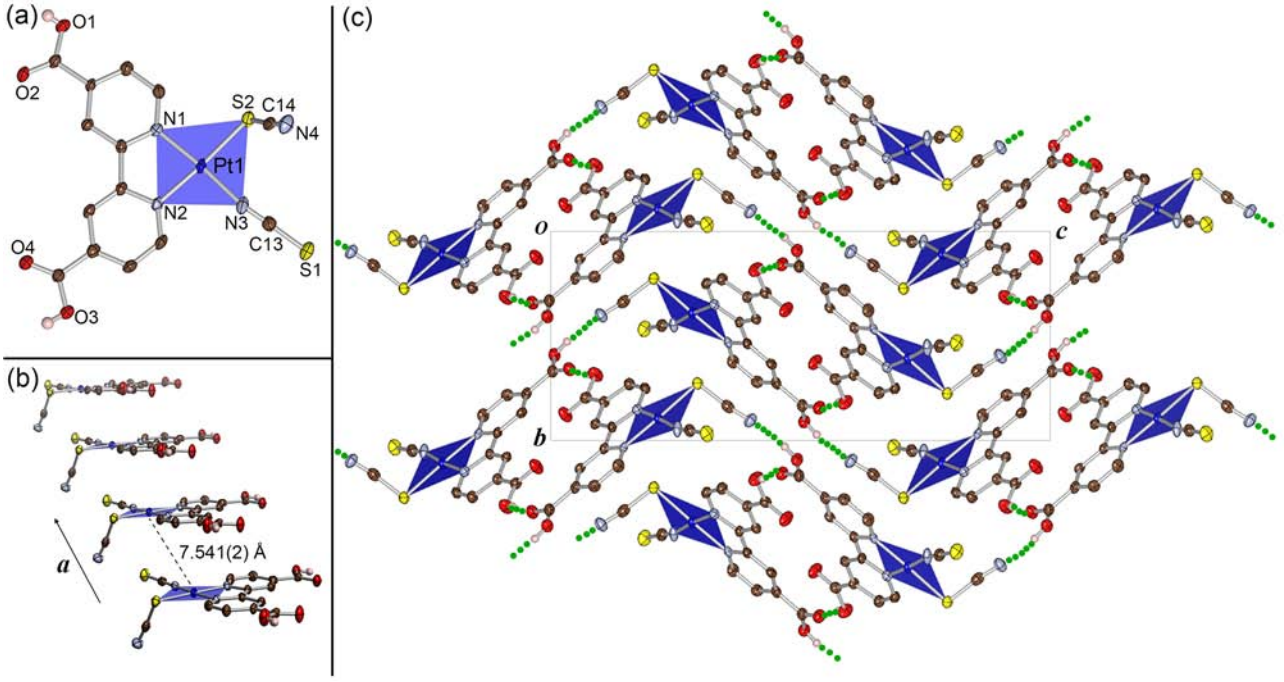

Figure 6. (a) Molecular structure, (b) 1-D stacked structure, and (c) packing diagram viewed down along the *a* axis of **1SN**. H atoms bonded to C are omitted for clarity. The coordination sphere of the Pt(II) ion is shown as the blue plane. Brown, light blue, red, and yellow ellipsoids, and pink balls represent C, N, O, S, and H atoms, respectively. Green dotted lines in (c) show the hydrogen bonds between **1SN** molecules.

respectively. This structure was similar to the nonsubstituted bipyridine complex [Pt(NCS)$_2$(bpy)],[23c,32c] which suggests that modification of the bipyridine ligand by two carboxyl groups has little effect on the intramolecular structure. In contrast, the carboxyl groups had a significant effect on both the intermolecular interactions and crystal structure. The crystal of **1NN·4DMF** includes four DMF solvent molecules, and two of the four DMF molecules form hydrogen bonds to the carboxyl groups (O4...O5 2.509(10) Å and O2...O6 2.497(8) Å), as shown in Figure 5(a). DMF inclusion results in intermolecular metallophilic interaction between Pt(II) ions being negligibly weak, as shown in Figure 5(b) (the shortest Pt−Pt distance is 6.893 Å). However, this yellow crystal of **1NN·4DMF** gradually changed to red after the samples were kept in air at room temperature for 1 d. These findings suggest that the solvated DMF molecules are easily removed, which may lead to a remarkable change in the intermolecular metallophilic and/or $\pi-\pi$ stacking interactions.

Figure 6(a) shows the molecular structure of **1SN**. X-ray structural analysis clearly indicated that one thiocyanate ligand was bound to the Pt(II) ion by the S atom and the other was coordinated by the N atom. The observed bond lengths and angles around the [Pt(SCN)(NCS)(H$_2$dcbpy)] molecule were similar to those of the nonsubstituted bipyridine complex [Pt(SCN)(NCS)(bpy)],[23c] except for the planarity of the molecule (Table S1 of the Supporting Information). Although all atoms of one [Pt(SCN)(NCS)(bpy)] molecule lie on the same plane, the S-coordinated thiocyanate ligand of **1SN** is directed up from the coordination plane (torsion angle N1−Pt1−S2−C14 = 117.3(2)°). This nonplanar structure of **1SN** prevents each molecule from forming a closely stacked columnar structure with effective metallophilic interactions between adjacent Pt(II) ions, as shown in Figure 6(b). As shown in Figure 6(c), one carboxyl group of **1SN** forms two types of hydrogen bonds. Specifically, one is with the N terminal of the S-coordinated SCN ligand, and the second is with the carboxyl group of the adjacent molecule. The other carboxyl group forms only one hydrogen bond with the carboxyl group of the adjacent molecule. As a result, an infinite ladder-type hydrogen-bond network is formed in **1SN**. In contrast to the solvent-included structure of **1NN·4DMF**, there is no solvent molecule in this crystal, despite the use of polar solvents (water and acetone) in the recrystallization.

Linkage Isomerization in Solution. As discussed above, the isomer with S-coordinated thiocyanato ligands, **1SS·H$_2$O**, was converted to **1SN** or **1NN·3DMF** by exposing it to acetone or DMF vapor, respectively. Surprisingly, exposure to DMF vapor resulted in all of the isomers, including the isomeric mixture being completely converted to **1NN·3DMF**, accompanied by DMF vapor adsorption. To clarify the origin of such a high conversion yield, the linkage isomerization behavior in the solution state was studied. Figure 7 shows the change in the ^{1}H NMR spectra of **1SS·H$_2$O** in DMF-d$_7$ solution during standing at room temperature. In the DMF solution state, the three proton signals that could be assigned to **1SS** were gradually decreased, while signals derived from **1SN** and **1NN** increased gradually. However, after 6 d, the isomerization reaction had already reached its equilibrium state, at which point the three proton signals assigned to **1NN,** as well as six proton signals of **1SN**, were observed. In the equilibrium state at room temperature, the isomeric ratio of the three isomers was estimated to be 63:36:1 = **1NN**:**1SN**:**1SS**. The same isomeric ratio was obtained from the linkage isomerization in the DMF-d$_7$ solution of **1NN·3DMF** (Figure S8 of the Supporting Information). These results suggest that linkage isomerization from the other isomers to **1NN** induced by DMF vapor in the solid state is not driven by any dissolution/recrystallization process in the DMF microdroplet on the crystal surface but by structural transformation involving DMF vapor adsorption. It is noted that the isomeric ratio at the

dx.doi.org/10.1021/ic202734f | *Inorg. Chem.* 2012, 51, 7508−7519

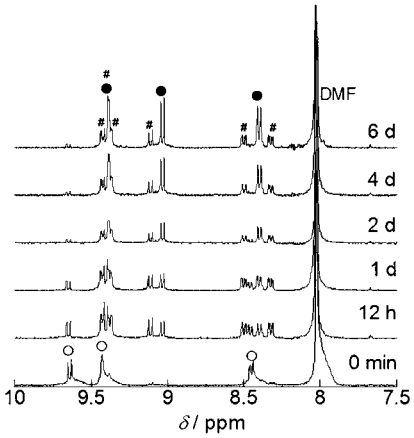

Figure 7. ^{1}H NMR spectral change of **1SS·H$_2$O** in DMF-d$_7$ solution (aromatic region) while standing at room temperature. The symbols ○, ●, and # indicate the signals for [Pt(SCN)$_2$(H$_2$dcbpy)], [Pt(NCS)$_2$(H$_2$dcbpy)], and [Pt(SCN)(NCS)(H$_2$dcbpy)], respectively.

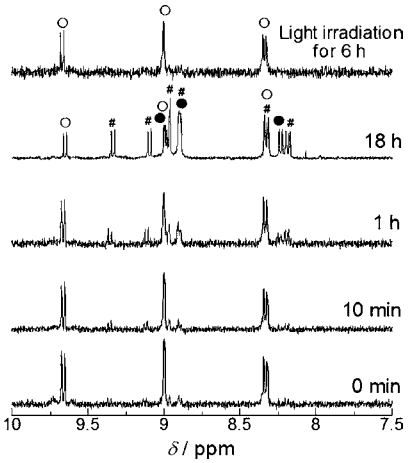

Figure 8. ^{1}H NMR spectral change of **1SS·H$_2$O** in MeOD solution (aromatic region) while standing at room temperature and after light irradiation for 6 h ($\lambda_{irr.}$ = 300 ± 10 nm). The symbols ○, ●, and # indicate the signals for [Pt(SCN)$_2$(H$_2$dcbpy)], [Pt(NCS)$_2$(H$_2$dcbpy)], and [Pt(SCN)(NCS)(H$_2$dcbpy)], respectively.

equilibrium state was almost independent of the solution temperature but the isomerization rate from **1SS** to the others strongly depends on the temperature (Figure S9 of the Supporting Information); the time to attain equilibrium state was estimated to be about 3 weeks at 278 K and 1 day at 323 K.

It is well known that the isomeric ratio of thiocyanato metal complexes in solution strongly depends on the hydrogen-bonding ability of the solvent molecule.[24b] In proton-donating solvents such as alcohols, isomers with S-coordinated thiocyanato ligands would be stabilized by forming hydrogen bonds between noncoordinated negatively charged N atoms of the thiocyanato ligand and the solvent molecule. As mentioned above, the linkage isomerizations from isomers containing the S-coordinated thiocyanato ligand to isomers with N-coordinated isothiocyanato ligands such as **1SS** to **1SN** or **1SN** to **1NN** have been achieved in the solid state by exposure to DMF and acetone vapors. However, complete inverse isomerizations from **1NN** or **1SN** to **1SS** have not been observed in the solid state. To investigate the possibility of complete inverse linkage isomerization, ^{1}H NMR spectral changes in MeOD solution were evaluated. As shown in Figure 8, proton signals of **1SS·H$_2$O** gradually decreased, and signals derived from the other linkage isomers increased as in the DMF-d$_7$ solution. It should be noted that the isomerization rate of **1SS** to the other isomers was remarkably larger in MeOD than that in DMF-d$_7$ (Figure S10 of the Supporting Information); the isomerization of **1SS** in MeOD at 278 K was found to reach its equilibrium state within 30 h, which is significantly shorter than that in DMF-d$_7$ at 278 K (about 3 weeks). In the equilibrium state after 18 h at room temperature, the isomeric ratio of the three isomers was estimated to be 42:42:16 = **1NN**:**1SN**:**1SS**; the isomeric ratio of the **1SS** was remarkably increased compared to that in DMF-d$_7$ solution. Thus, as expected, isomers having the S-coordinated thiocyanato ligands **1SS** and **1SN** were more stable in MeOD than in DMF, which was probably the result of hydrogen-bond formation with the MeOD molecule. Interestingly, a drastic change was observed in response to UV light irradiation ($\lambda_{irr.}$ = 300 ± 10 nm) of the solution in the equilibrium state. All signals originating from both **1NN** and **1SN** disappeared completely, and only three proton signals assigned to **1SS** were observed after light irradiation for 6 h. When photoirradiation was conducted using blue light ($\lambda_{irr.}$ = 400 ± 10 nm), the isomerization occurred much more slowly. Such photoinduced ^{1}H NMR spectral change was never observed under exposure to light with wavelengths above 500 nm. Considering that no absorption band was observed at 500 nm in the isomeric mixture in MeOH solution (Figure S11 of the Supporting Information), these wavelength-dependent spectral changes clearly indicate that photoinduced inverse linkage isomerizations from **1NN** or **1SN** to **1SS** occur in MeOD solution.

Possible Mechanism of Vapor-Induced Linkage Isomerization. Observed linkage isomerizations of **1** are summarized in Scheme 2 with the schematic energy diagram of each linkage isomer. As discussed above, these interesting vapor-induced linkage isomerizations in the solid state depended on the type of vapor, despite each pure isomer gradually being changed to a mixture of three isomers in the solution state. In this section, we discuss the possible mechanism of this vapor-induced linkage isomerization in the solid state.

Because the bis(thiocyanato)−Pt(II) complex with the nonsubstituted bipyridine ligand, [Pt(*thiocyanato*)$_2$(bpy)], did not show any vapor-induced linkage isomerization in the solid state,[23c] the carboxyl group of the H$_2$dcbpy ligand is believed to play an important role in the vapor-induced linkage isomerization reactions. It should be noted that two isomers having the S-coordinated thiocyanato ligand, [Pt(SCN)$_2$(bpy)] and [Pt(SCN)(NCS)(bpy)], were gradually converted to an isomer containing only the N-coordinated isothiocyanato ligand, [Pt(NCS)$_2$(bpy)], at 75 °C, whereas those having the H$_2$dcbpy ligands, **1SS** and **1SN**, were never converted to the other isomers, even under the same conditions. These differences imply that the intermolecular hydrogen bonds between the carboxyl group of the H$_2$dcbpy and the thiocyanato ligand play an important role in stabilization of the isomers having the S-coordinated thiocyanato ligand. Hydrogen-bond formation between the N atom of the thiocyanato ligand and proton-donating molecules is well known to stabilize the S-coordinated isomer more effectively than the N-coordinated isomer because of the stronger hydrogen-bonding ability of the more electronegative N atom

dx.doi.org/10.1021/ic202734f | Inorg. Chem. 2012, 51, 7508−7519

Scheme 2. Summary of Vapor- and Photoinduced Isomerization of 1. (Bottom): Energy Diagram of Each Isomer in the Solid State

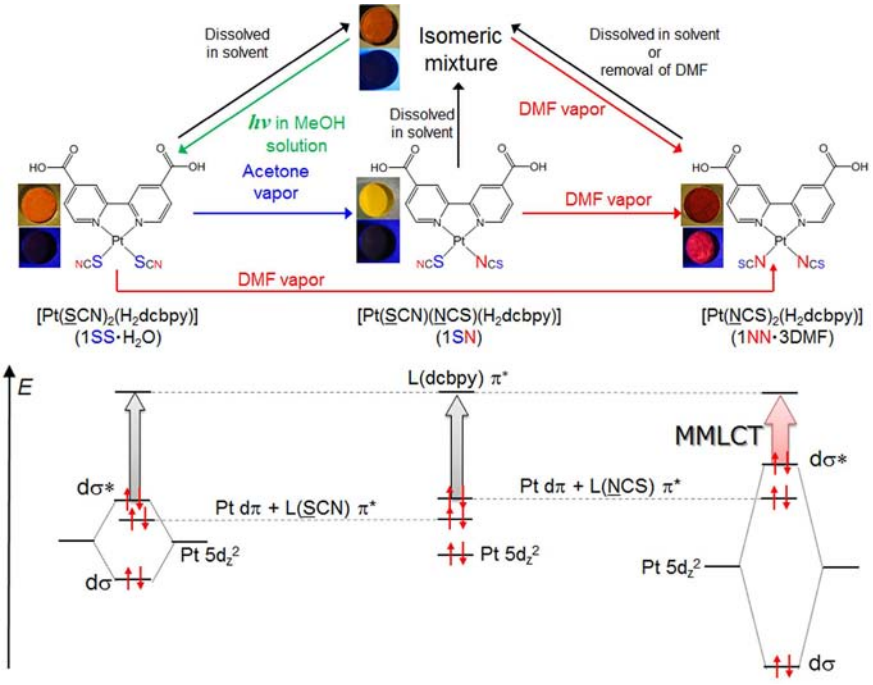

of the thiocyanato ligand than that of the S atom of the isothiocyanato ligand.[21] A two-dimensional hydrogen-bonded sheet structure is formed in the bis(cyano)−Pt(II) complex with the H_2dcbpy ligand $[Pt(CN)_2(H_2dcbpy)]$;[3c] therefore, it is possible that a similar hydrogen-bonded network structure, as shown in Scheme 3(a), is formed in **1SS·H_2O**.

The intermolecular hydrogen-bonded network formed in **1SS·H_2O** also suggests a possible mechanism of the vapor-induced linkage isomerization of **1**. Table 2 shows the relationship between the isomerization reaction induced by vapor and the donor number of the vapor molecule. It is interesting to note that the isomerization from **1SS·H_2O** to **1NN·*n*(vapor)** occurs upon exposure to vapors with donor numbers above 26, and that vapors with moderate donor numbers of around 10 promoted isomerization of **1SS·H_2O** to **1SN**. Vapors with very small donor numbers did not induce any isomerization reaction in the solid state. This donor number dependence can be explained by hydrogen-bond formation between the carboxyl group of the H_2dcbpy ligand and the exposed vapor molecule. It is well known that molecules with large donor numbers can form strong hydrogen bonds with proton-donating molecules that contain carboxyl and/or hydroxy groups.[33] Therefore, vapors such as DMF would be easily adsorbed into the crystal lattice of **1SS·H_2O**, and this adsorption is accompanied by breaking of the hydrogen-bonded network structure and subsequent hydrogen-bond formation between the vapor molecule and the carboxyl group of **1SS**. In fact, the energy (1653 cm^{-1}) of the ν(C═O) stretching mode of the DMF molecule in **1NN·3DMF** was shifted to a wavenumber about 22 cm^{-1} lower than that of the normal DMF liquid (1675 cm^{-1}), while the ν(C═O) stretching mode of the carboxyl group of H_2dcbpy in **1NN·3DMF** was also shifted to a wavenumber about 10 cm^{-1} lower than that in **1SS·H_2O** (see above). These results provide clear evidence of hydrogen-bond formation between the carboxyl group and adsorbed DMF molecule. In such a vapor-adsorbed structure, stabilization of S-coordinated isomers given by the intermolecular hydrogen bond should disappear because the carboxyl groups of the H_2dcbpy ligand have already hydrogen-bonded to

Scheme 3. Possible Mechanism of the DMF-Vapor-Induced Linkage Isomerization from (a) 1SS·H_2O to (b) 1NN·3DMF, Accompanied by Rearrangement of Hydrogen Bonds

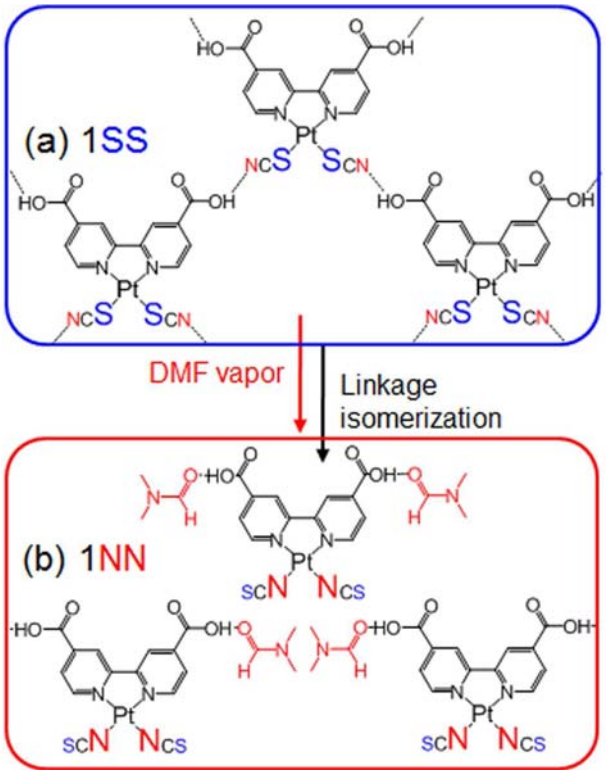

dx.doi.org/10.1021/ic202734f | Inorg. Chem. 2012, 51, 7508−7519

Table 2. Vapor-Induced Linkage Isomerization of 1SS and Donor Numbers of Vapor Molecules

vapor	DN[a]	obtained isomer(s)	color of solid	color of luminescence
DMSO	29.8	**1NN·*n*DMSO**	yellow	orange
DMA	27.8	**1NN·*n*DMA**	yellow	orange
DMF	26.6	**1NN·3DMF**	red	red
MeOH	23.5	**1SN+1NN**	reddish-yellow	orange
EtOH	20.0	**1SN+1NN**[b]	yellow	orange
acetone	17.0	**1SN**[b]	Yellow	–
CH_3CN	14.1	**1SN**[b]	yellow	–
CH_2Cl_2	-	**1SN**[b]	yellow	
$CHCl_3$	4.0	**1SN**[b]	yellow	–
n-hexane	0	no change	orange	–
cyclohexane	0	no change	orange	–

[a]See ref 33. [b]These samples contains about 20% **1SS** as an impurity.

the vapor molecules. Consequently, linkage isomerization from kinetically favorable **1SS·H_2O** to thermodynamically favorable **1NN·3DMF** could occur (Scheme 3(b)). On the other hand, highly polar and protic solvent vapors such as MeOH and EtOH also promote linkage isomerization, but the dominant isomer was not **1NN** but **1SN**. Because these alcohols can act as both proton-donating and -accepting molecules because of their hydroxyl group, the S-coordinated isomers would be stabilized by hydrogen bonds with not only with the carboxyl groups of H_2dcbpy ligand but also with the adsorbed alcohols. Consequently, under exposure to these alcohols, the linkage isomerization reaction from **1SS** to **1SN** would be promoted more dominantly than that from **1SS** to **1NN**.

These linkage isomerization reactions should involve the significant change of the molecular shape, that is, all the three atoms of N-coordinated isothiocyanato ligand should be placed in the coordination plane of Pt(II) ion because of the effective π-back bonding between Pt(II) ion and the isothiocyanato ligand. On the other hand, the S atom of thiocyanate ligand has three lone pairs, which make the ligand possible to be directed up or down from the coordination plane. In fact, the thiocyanate ligands of [Pt(SCN)$_2$(bpy)] are directed up and down from the coordination plane, whereas the isothiocyanato ligands of [Pt(NCS)$_2$(bpy)] and **1NN·4DMF** are bonded in the linear coordination fashion.[23c] Thus, the planar molecule of **1NN** could easily form one-dimensional stacked columnar structure, resulting in the effective intermolecular metallophilic interaction between Pt(II) ions. Conversely, the intermolecular metallophilic interaction in the **1SS·H_2O** is expected to be weaker than that of **1NN·3DMF** due to the bent structure. Considering the fact that the UV−vis spectrum of **1SS·H_2O** in DMF solution was very similar to that of **1NN·3DMF** (Figure S12 of the Supporting Information), the intermolecular metallophilic interaction in the solid state probably plays the important role on the emission and absorption properties of three isomers, i.e., the nonemissive **1SS·H_2O** and emissive **1NN·3DMF**.

Conversely, nonpolar vapors such as *n*-hexane cannot form such a hydrogen bond, resulting in no isomerization. It should be emphasized that the **1NN** isomer was not necessarily the most stable isomer among the three possible isomers in the environment without DMF vapor because **1NN·3DMF** was converted to an isomeric mixture by removal of the adsorbed DMF. The isomeric ratio (**1SS**:**1SN**:**1NN** = 5:68:27) suggests that **1SN** may be more stable than **1NN** in the no-vapor-adsorbed state. Conversely, the isomerization from **1SS·H_2O** to **1SN** induced by moderate polar vapors should be derived from a different mechanism because the obtained **1SN** did not adsorb any vapor molecules. Considering that **1SS·H_2O** contains about 1 mol mol^{-1} hydrated water molecules, whereas **1SN** does not contain any water or vapor molecules, the dehydration of **1SS·H_2O** is an important step in promotion of linkage isomerization from **1SS·H_2O** to **1SN**. Thus, moderate polar vapors may promote this dehydration step, accompanied by the isomerization from **1SS·H_2O** to the more themodynamically favorable **1SN**. Considering the facts that there is no intermolecular metallophilic interaction in **1SN** crystal and UV−vis spectra of the three isomers in DMF-solutions are quite similar to each other (Figure S12 of the Supporting Information), the moderate color change in the vapor-induced linkage isomerization from **1SS·H_2O** to **1SN** would also originate from the change of intermolecular metallophilic and/or $\pi-\pi$ stacking interactions. The minor residual **1SS** in the **1SN** sample obtained by exposing **1SS·H_2O** to acetone, CH_3CN or $CHCl_3$ may be the result of incomplete dehydration and/or low affinity of these vapors for the hydrogen-bonded network structure of **1SS·H_2O**.

CONCLUSION

We successfully synthesized a new Pt(II)−diimine complex with an ambidentate thiocyanato (SCN^-) ligand, [Pt(*thiocyanato*)$_2$(H_2dcbpy)] (**1**), and found that complex **1** is a new class of vapochromic system, originating from both the linkage isomerization of the thiocyanato ligand and the change in intermolecular metallophilic interaction. The isomer with S-coordinated thiocyanato ligands, [Pt(SCN)$_2$(H_2dcbpy)] (**1SS·H_2O**), was purely synthesized by reaction of the starting complex, [$PtCl_2$(H_2dcbpy)], with potassium thiocyanate at 0 °C. **1SS·H_2O** is converted completely to one isomer with N-coordinated isothiocyanato ligands, [Pt(NCS)$_2$(H_2dcbpy)]·**3DMF** (**1NN·3DMF**), in the solid state simply by exposure to DMF vapor at room temperature for 1 d, whereas the conversion of **1SS·H_2O** in solution state provides an isomeric mixture of the three possible linkage isomers. Upon exposure of **1SS·H_2O** to acetone vapor at room temperature for 1 d, about 80% of **1SS·H_2O** is converted to an isomer having both the S- and N-coordinated thiocyanato ligands, [Pt(SCN)(NCS)(H_2dcbpy)] (**1SN**). **1SN** is also converted to **1NN·3DMF** by exposing it to DMF vapor at room temperature for 1 d. The differences in the hydrogen-bonding manner of the crystal structures of **1SN** and **1NN·4DMF** suggest that the stability of each isomer is strongly affected by the hydrogen bonds formed at the carboxyl groups of the H_2dcbpy ligand. In these vapor-induced linkage isomerization reactions, significant color changes and ON−OFF switching of the luminescence were observed, specifically, nonluminescent orange **1SS·H_2O** to luminescent red **1NN·3DMF** and to nonluminescent yellow **1SN**. These vapor-induced linkage isomerizations in the solid state strongly depend on the donor number of the vapor molecules, suggesting that the complex can recognize differences in the vapor molecules that may be applicable to vapor-selective sensors and/or vapor indicators. The **1NN** isomer was successfully converted to **1SS** in methanol solution under UV light irradiation. Further studies to develop other linkage isomerization systems driven by exposure to VOC vapors in the solid state are now in progress.

dx.doi.org/10.1021/ic202734f | *Inorg. Chem.* 2012, 51, 7508−7519

■ ASSOCIATED CONTENT

Supporting Information

X-ray crystallographic files of **1SN** and **1NN·4DMF** in CIF format; Thermogravimetric analyses of **1NN·3DMF** and **1SN**; ^{1}H NMR spectra of **1SN** after heating to 150 °C; Change of the PXRD pattern of **1SN** in DMF vapor; IR spectra of **1SN** obtained by exposing **1SS·H_2O** to $CHCl_3$ and CN_3CN; ^{1}H NMR spectra of the samples obtained by exposing **1SS·H_2O** to DMSO, DMA, MeOH and EtOH vapor; Excitation and Emission spectra of **1NN** samples obtained by **1SS·H_2O** to DMA or DMSO vapors; ^{1}H NMR spectral changes of **1NN·3DMF** in DMF-d_7 solution; Time and temperature dependences of the ^{1}H NMR spectrum of **1SS·H_2O** in DMF-d_7 and MeOD-d_4 solutions; and UV−vis absorption spectra of **1SS·H_2O** and isomeric mixture in MeOH solution. These materials are available free of charge via the Internet at http://pubs.acs.org.

■ AUTHOR INFORMATION

Corresponding Author

*Phone: +81-11-706-3819 (A.K.), +81-11-706-3817 (M.K.). Fax: +81-11-706-3447 (A.K.), +81-11-706-3447 (M.K.). E-mail: akoba@sci.hokudai.ac.jp (A.K.), mkato@sci.hokudai.ac.jp (M.K.).

Notes

The authors declare no competing financial interest.

■ ACKNOWLEDGMENTS

This study was supported by a Grant-in-Aid for Scientific Research (B)(23350025), Photochromism (No. 471), Coordination Programming (No. 2107), Young Scientists (B) (24750049), and the Global COE Program (Project No. B01: Catalysis as the Basis for Innovation in Materials Science) from MEXT, Japan.

■ REFERENCES

(1) (a) De Silva, A. P.; Fox, D. B.; Huxley, A. J.M.; Moody, T. S. *Coord. Chem. Rev.* **2000**, *205*, 41−57. (b) Prodi, L.; Bolletta, F.; Montalti, M.; Zaccheroni, N. *Coord. Chem. Rev.* **2000**, *205*, 59−83. (c) Fabbrizzi, L.; Licchelli, M.; Rabaioli, G.; Taglietti, A. *Coord. Chem. Rev.* **2000**, *205*, 85−108. (d) Parker, D. *Coord. Chem. Rev.* **2000**, *205*, 109−130. (e) Beer, P. D.; Cadman, J. *Coord. Chem. Rev.* **2000**, *205*, 131−155. (f) Robertson, A.; Shinkai, S. *Coord. Chem. Rev.* **2000**, *205*, 157−199. (g) Keefe, M. H.; Benkstein, K. D.; Hupp, J. T. *Coord. Chem. Rev.* **2000**, *205*, 201−228. (h) Demas, J. N.; DeGraff, B. A. *Coord. Chem. Rev.* **2001**, *211*, 317−351. (i) Sun, S.-S; Lees, A. J. *Coord. Chem. Rev.* **2002**, *230*, 170−191. (j) Kato, M. *Bull. Chem. Soc. Jpn.* **2007**, *80*, 287−294.

(2) Magnus-type Pt(II) complexes: (a) Exstrom, C. L.; Sowa, J. R., Jr.; Daws, C. A.; Janzen, D.; Mann, K. R. *Chem. Mater.* **1995**, *7*, 15−17. (b) Daws, C. A.; Exstrom, C. L.; Sowa, J. R., Jr.; Mann, K. R. *Chem. Mater.* **1997**, *9*, 363−368. (c) Exstrom, C. L.; Pomije, M. K.; Mann, K. R. *Chem. Mater.* **1998**, *10*, 942−945. (d) Drew, S. M.; Janzen, D. E.; Buss, C. E.; MacEwan, D. I.; Dublin, K. M.; Mann, K. R. *J. Am. Chem. Soc.* **2001**, *123*, 8414−8415. (e) Grate, J. W.; Moore, L. K.; Janzen, D. E.; Veltkamp, D. J.; Kaganove, S.; Drew, S. M.; Mann, K. R. *Chem. Mater.* **2002**, *14*, 1058−1066.

(3) Neutral mononuclear Pt(II) complexes: (a) Buss, C. E.; Mann, K. R. *J. Am. Chem. Soc.* **2002**, *124*, 1031−1039. (b) Wadas, T. J.; Wang, Q.-M.; Kim, Q.-M.; Flaschenreim, C.; Blanton, T. N.; Eisenberg, R. *J. Am. Chem. Soc.* **2004**, *126*, 16841−16849. (c) Kato, M.; Kishi, S.; Wakamatsu, Y.; Sugi, Y.; Osamura, Y.; Koshiyama, T.; Hasegawa, M. *Chem. Lett.* **2005**, *34*, 1368−1369. (d) Dylla, A. G.; Janzen, D. E.; Pomije, M. K.; Mann, K. R. *Organometallics* **2007**, *26*, 6243−6247. (e) Ni, J.; Wu, Y.-H.; Zhang, X.; Li, B.; Zhang, L.-Y.; Chen, Z.-N. *Inorg. Chem.* **2009**, *48*, 10202−10210. (f) Ni, J.; Zhang, L.-Y.; Wen, H.-M.; Chen, Z.-N. *Chem. Commun.* **2009**, 3801−3803. (g) Ni, J.; Zhang, X.; Wu, Y.-H.; Zhang, L.-Y.; Chen, Z.-N. *Chem.—Eur. J.* **2011**, *17*, 1171−1183.

(4) Cationic mononuclear Pt(II) complexes: (a) Grove, L. J.; Rennekamp, J. M.; Jude, H.; Connick, W. B. *J. Am. Chem. Soc.* **2004**, *126*, 1594−1595. (b) Du., P.; Schneider, J.; Brennessel, W. W.; Eisenberg, R. *Inorg. Chem.* **2008**, *47*, 69−77. (c) Muro, M. L.; Daws, C. A.; Castellano, F. N. *Chem. Commun.* **2008**, 6134−6136. (d) Grove, L. J.; Oliver, A. G.; Krause, J. A.; Connick, W. B. *Inorg. Chem.* **2008**, *47*, 1408−1410. (e) Kobayashi, A.; Fukuzawa, Y.; Noro, S.; Nakamura, T.; Kato, M. *Chem. Lett.* **2009**, *38*, 998−999. (f) Field, J. S.; Grimmer, C. D.; Munro, O. Q.; Waldron, B. P. *Dalton Trans.* **2010**, *39*, 1558−1567. (g) Mathew, I.; Sun, W. *Dalton Trans.* **2010**, *39*, 5885−5898.

(5) Anionic mononuclear Pt(II) complexes: Forniés, J.; Fuertes, S.; López, J. A.; Martín, A.; Sicilia, V. *Inorg. Chem.* **2008**, *47*, 7166−7176.

(6) Dinuclear Pt(II) complexes: (a) Kato, M.; Omura, A.; Toshikawa, A.; Kishi, S.; Sugimoto, Y. *Angew. Chem., Int. Ed.* **2002**, *41*, 3183−3185. (b) Kui, S. C. F.; Chui, S. S.-Y.; Che, C.-M.; Zhu, N. *J. Am. Chem. Soc.* **2006**, *128*, 8297−8309.

(7) Coordination polymers: (a) Matsuzaki, H.; Kishida, H.; Okamoto, H.; Takizawa, K.; Matsunaga, S.; Takaishi, S.; Miyasaka, H.; Sugiura, K.; Yamashita, M. *Angew. Chem., Int. Ed.* **2005**, *44*, 3240−3243. (b) Kobayashi, A.; Hara, H.; Noro, S.; Kato, M. *Dalton Trans.* **2010**, *39*, 3400−3406.

(8) (a) Vickery, J. C.; Olmstead, M. M.; Fung, E. Y.; Balch, A. L. *Angew. Chem., Int. Ed.* **1997**, *36*, 1179−1181. (b) Mansour, M. A.; Connick, W. B.; Lachicotte, R. J.; Grsling, H. J.; Eisenberg, R. *J. Am. Chem. Soc.* **1998**, *120*, 1329−1330. (c) Lefebvre, J.; Batchelor, R. J.; Leznoff, D. B. *J. Am. Chem. Soc.* **2004**, *126*, 16117−16125. (d) Rawashdeh-Omary, M. A.; Rashdan, M. D.; Dharanipathi, S.; Elbjeirami, O.; Ramesh, P.; Dias, H. V. R. *Chem. Commun.* **2011**, *47*, 1160−1162.

(9) (a) Dong, Y.; Lam, J. W. Y.; Li, Z.; Qin, A.; Tong, H.; Dong, Y.; Feng, X.; Tang, B. Z. *J. Inorg. Organomet. Polym. Mater.* **2005**, *15*, 287−291. (b) Yoon, S.-J.; Chung, J. W.; Gierschner, J.; Kim, K. S.; Choi, M.-G.; Kim, D.; Park, S. Y. *J. Am. Chem. Soc.* **2010**, *132*, 13675−13683. (c) Takahashi, E.; Takaya, H.; Naota, T. *Chem.—Eur. J.* **2010**, *16*, 4793−4802. (d) Dou, C.; Chen, D.; Iqbal, J.; Yuan, Y.; Zhang, H.; Wang, Y. *Langmuir* **2011**, *27*, 6323−6329.

(10) (a) Kojima, M.; Taguchi, H.; Tsuchimoto, M.; Nakajima, K. *Coord. Chem. Rev.* **2003**, *237*, 183−186. (b) Mizukami, S.; Houjou, H.; Sugaya, K.; Koyama, E.; Tokuhisa, H.; Sasaki, T.; Kanesato, M. *Chem. Mater.* **2005**, *17*, 50−56. (c) Kobayashi, A.; Dosen, M.; Chang, M.; Nakajima, K.; Noro, S.; Kato, M. *J. Am. Chem. Soc.* **2010**, *132*, 15286−15298. (d) Chang, M.; Kobayashi, A.; Nakajima, K.; Chang, H.-C.; Kato, M. *Inorg. Chem.* **2011**, *50*, 8308−8317.

(11) Co complexes: (a) Beauvais, L. G.; Shores, M. P.; Long, J. R. *J. Am. Chem. Soc.* **2000**, *122*, 2763−2772. (b) Bradshw, D.; Warren, J. E.; Rosseinsky, M. J. *Science* **2007**, *315*, 977−980. (c) Boonmak, J.; Nakano, M.; Chaichit, N.; Pakawatchai, C.; Youngme, S. *Dalton Trans.* **2010**, *39*, 8161−8167.

(12) Ni complexes: Baho, N.; Zargarian, D. *Inorg. Chem.* **2007**, *46*, 299−308.

(13) Cu complexes: (a) Cariati, E.; Bu, X.; Ford, P. C. *Chem. Mater.* **2000**, *12*, 3385−3391. (b) Yamada, K.; Yagishita, S.; Tanaka, H.; Tohyama, K.; Adachi, K.; Kaizaki, S.; Kumagai, H.; Inoue, K.; Kitaura, R.; Chang, H.-C.; Kitagawa, S.; Kawata, S. *Chem.—Eur. J.* **2004**, *10*, 2647−2660. (c) Yamada, K.; Tanaka, H.; Yagishita, S.; Adachi, K.; Uemura, T.; Kitagawa, S.; Kawata, S. *Inorg. Chem.* **2006**, *45*, 4322−4324. (d) Bencini, A.; Casarin, M.; Forrer, D.; Franco, L.; Garau, F.; Masciocchi, N.; Pandolfo, L.; Pettinari, C.; Ruzzi, M.; Vittadini, A. *Inorg. Chem.* **2009**, *48*, 4044−4051.

(14) Au complexes: (a) Fernández, E. J.; López-de-Luzuriaga, J. M.; Monge, M.; Olmos, M. E.; Pérez, J.; Laguna, A.; Mohamed, A. A.; Fackler, J. P., Jr. *J. Am. Chem. Soc.* **2003**, *125*, 2022−2023. (b) Fernández, E. J.; López-de-Luzuriaga, J. M.; Monge, M.; Montiel, M.; Olmos, M. E.; Pérez, J. *Inorg. Chem.* **2004**, *43*, 3573−

3581. (c) Luquin, A.; Bariáin, C.; Vergara, E.; Cerrada, E.; Garrido, J.; Matias, I. R.; Laguna, M. *Appl. Organometal. Chem.* **2005**, *19*, 1232−1238. (d) Fernández, E. J.; López-de-Luzuriaga, J. M.; Monge, M.; Olmos, M. E.; Puelles, R. C.; Laguna, A.; Mohamed, A. A.; Fackler, J. P., Jr. *Inorg. Chem.* **2008**, *47*, 8069−8076. (e) Laguna, A.; Lasanta, T.; Lopez-de-Luzuriaga, J. M.; Monge, M.; Naumov, P.; Olmos, M. E. *J. Am. Chem. Soc.* **2010**, *132*, 456−457. (f) Strasser, C. E.; Catalano, V. J. *J. Am. Chem. Soc.* **2010**, *132*, 10009−10011. (g) Osawa, M.; Kawata, I.; Igawa, S.; Hoshino, M.; Fukunaga, T.; Hashizume, D. *Chem.—Eur. J.* **2010**, *16*, 12114−12126.

(15) The others: (a) Albrecht, M.; Lutz, M.; Spek., A. L.; Koten, G. V. *Nature* **2000**, *406*, 970−974. (b) Forniés, J.; Sicilia, V.; Casas, J. M.; Martín, A.; López, J. A.; Larraz, C.; Borja, P.; Ovejero, C. *Dalton Trans.* **2011**, *40*, 2898−2912.

(16) (a) Meinershagen, J. L.; Bein, T. *J. Am. Chem. Soc.* **1999**, *121*, 448−449. (b) Lu, W.; Chan, M. C. W.; Zhu, N.; Che, C.-M.; He, Z.; Wong, K.-Y. *Chem.—Eur. J.* **2003**, *9*, 6155−6166. (d) McManus, G. J.; Perry, J. J., IV; Perry, M.; Wagner, B. D.; Zaworotko, M. J. *J. Am. Chem. Soc.* **2007**, *129*, 9094−9101. (f) Liu, Z.; Bian, Z.; Bian, J.; Li, Z.; Nie, D.; Huang, C. *Inorg. Chem.* **2008**, *47*, 8025−8030. (g) McGee, K. A.; Marquardt, B. J.; Mann, K. R. *Inorg. Chem.* **2008**, *47*, 9143−9145. (h) Abe, T.; Suzuki, T.; Shinozaki, K. *Inorg. Chem.* **2010**, *49*, 1794−1800. (i) Stylianou, K. C.; Heck, R.; Chong, S. Y.; Bacsa, J.; Jones, J. T. A.; Khimyak, Y. Z.; Bradshaw, D.; Rosseinsky, M. J. *J. Am. Chem. Soc.* **2010**, *132*, 4119−4130. (j) Hudson, Z. M.; Sun, C.; Harris, K. J.; Lucier, B. E. G.; Schurko, R. W.; Wang, S. *Inorg. Chem.* **2011**, *50*, 3447−3457. (k) Lee, C.-S.; Zhuang, R. R.; Sabiah, S.; Wang, J.-C.; Hwang, W.-S.; Lin, I. J. B. *Organometallics* **2011**, *30*, 3897−3900.

(17) (c) Matsushima, R.; Nishimura, N.; Goto, K.; Kohno, Y. *Bull. Chem. Soc. Jpn.* **2003**, *76*, 1279−1283. (e) Vaidya, S.; Johnson, C.; Wang, X.-Y.; Schmehl, R. H. *J. Photochem. Photobiol. A* **2007**, *187*, 258−262.

(18) (a) Sudesh Kumar, G.; Neckers, D. C. *Chem. Rev.* **1989**, *89*, 1915−1925. (b) Liu, Z. F.; Hashimoto, K.; Fujishima, A. *Nature* **1990**, *347*, 658−660. (c) Ikeda, T.; Tsutsumi, O. *Science* **1995**, *268*, 1873−1875. (d) Ichimura, K.; Oh, S.-K.; Nakagawa, M. *Science* **2000**, *288*, 1624−1626. (e) Natansohn, A.; Rochon, P. *Chem. Rev.* **2002**, *102*, 4139−4176.

(19) (a) Irie, M.; Mohri, M. *J. Org. Chem.* **1988**, *53*, 803−808. (b) Irie, M.; Kobatake, S.; Horichi, M. *Science* **2001**, *291*, 1769−1772. (c) Tian, H.; Yang, S. *Chem. Soc. Rev.* **2004**, *33*, 85−97. (d) Matsuda, K.; Irie, M. *J. Photochem. Photobiol. C* **2004**, *5*, 169−182.

(20) (a) Sakamoto, R.; Murata, M.; Kume, S.; Sampei, H.; Sugimoto, M.; Nishihara, H. *Chem. Commun.* **2005**, 1215−1217. (b) Sakamoto, R.; Kume, S.; Sugimoto, M.; Nishihara, H. *Chem.—Eur. J.* **2009**, *15*, 1429−1439. (c) Hasegawa, Y.; Kume, S.; Nishihara, H. *Dalton Trans.* **2009**, 280−284.

(21) Reviews: (a) Bailey, R. A.; Kozak, S. L.; Michelsen, T. W.; Mills, W. N. *Coord. Chem. Rev.* **1971**, *6*, 407−445. (b) Kawaguchi, S. *Variety in Coordination Modes of Ligands in Metal Complexes*; Springer-Verlag: Berlin, 1988.

(22) Pd complexes: (a) Basolo, F.; Burmeister, J. L. *J. Am. Chem. Soc.* **1963**, *85*, 1700−1701. (b) Burmeister, J. J.; Basolo, F. *Inorg. Chem.* **1964**, *3*, 1587−1593. (c) Basolo, F.; Baddley, W. H.; Weidenbaum, K. J. *J. Am. Chem. Soc.* **1966**, *88*, 1576−1578. (d) Meek, D. W.; Nicpon, P. E.; Meek, V. I. *J. Am. Chem. Soc.* **1970**, *92*, 5351−5359. (e) Burmeister, J. L.; Hassel, R. L.; Phelan, R. J. *Inorg. Chem.* **1971**, *10*, 2032−2038. (f) Palenik, G. J.; Mathew, M.; Steffen, W. L.; Beran, G. *J. Am. Chem. Soc.* **1975**, *97*, 1059−1066.

(23) Pt complexes : (a) Coyer, M. J.; Croft, M.; Chen, J.; Herber, R. H. *Inorg. Chem.* **1992**, *31*, 1752−1757. (b) Coyer, M. J.; Herber, R. H.; Chen, J.; Croft, M.; Szu, S. P. *Inorg. Chem.* **1994**, *33*, 716−721. (c) Kishi, S.; Kato, M. *Inorg. Chem.* **2003**, *42*, 8728−8734.

(24) The others: (a) Melpolder, J. B.; Burmeister, J. L. *Inorg. Chim. Acta* **1975**, *15*, 91−104. (b) Maronery, M. J.; Fey, E. O.; Baldwin, D. A.; Stenkamp, R. E.; Jensen, L. H.; Rose, N. J. *Inorg. Chem.* **1986**, *25*, 1409−1414. (c) Jurisson, S.; Halihan, M. M.; Lydon, J. D.; Barnes, C. L.; Nowotnik, D. P.; Nunn, A. D. *Inorg. Chem.* **1998**, *37*, 1922−1928.

(25) Islam, A.; Sugihara, H.; Hara, K.; Singh, L. P.; Katoh, R.; Yanagida, M.; Takahashi, Y.; Murata, S.; Arakawa, H.; Fujihashi, G. *Inorg. Chem.* **2001**, *40*, 5371−5380.

(26) *CrystalClear*; Molecular Structure Corporation: Orem, UT, 2001.

(27) SIR2004: Burla, M. C.; Caliandro, R.; Camalli, M.; Carrozzini, B.; Cascarano, G. L.; De Caro, L.; Giacovazzo, C.; Polidori, G.; Spagana, R. *J. Appl. Crystallogr.* **2005**, *38*, 381−388.

(28) SHLEX97 ; Sheldrick, G. M. *Acta Crystallogr., Sect. A* **2008**, *64*, 112−122.

(29) *CrystalStructure 3.7.0*, Crystal Structure Analysis Package; Rigaku and Rigaku/MSC, 2000−2005.

(30) Mononuclear complexes: (a) Miskowski, V. M.; Houlding, V. H. *Inorg. Chem.* **1989**, *28*, 1529−1533. (b) Houlding, V. H.; Miskowski, V. M. *Coord. Chem. Rev.* **1991**, *111*, 145−152. (c) Miskowski, V. M.; Houlding, V. H. *Inorg. Chem.* **1991**, *30*, 4446−4452. (d) Miskowski, V. M.; Houlding, V. H.; Che, C.-M.; Wang, Y. *Inorg. Chem.* **1993**, *32*, 2518−2524. (e) Kato, M.; Kosuge, C.; Morii, K.; Ahn, J. S.; Kitagawa, H.; Mitani, T.; Matsushita, M.; Kato, T.; Yano, S.; Kimura, M. *Inorg. Chem.* **1999**, *38*, 1638−1641. (f) Connick, W. B.; Henling, L. M.; Marsh, R. E.; Gray, H. B. *Inorg. Chem.* **1996**, *35*, 6261−6265. (g) Cummings, S. D.; Eisenberg, R. *J. Am. Chem. Soc.* **1996**, *118*, 1949−1960. (h) Kwok, W. M.; Phillips, D. L.; Yeung, P. K,-Y.; Yam, V. W.-W. *Chem. Phys. Lett.* **1996**, *262*, 699−708. (i) Lai, S.-W.; Lam, H.-W.; Lu, W.; Cheung, K.-K.; Che, C.-M. *Organometallics* **2002**, *21*, 226−234. (j) Pomestchenko, I. E.; Castellano, F. N. *J. Phys. Chem. A* **2004**, *108*, 3485−3492. (k) Wong, K. M.-C.; Yam, V. W.-W. *Coord. Chem. Rev.* **2007**, *251*, 2477−2488.

(31) Dinuclear complexes: (a) Koshiyama, T.; Omura, A.; Kato, M. *Chem. Lett.* **2004**, *33*, 1386−1387. (b) Ma, B.; Li, J.; Djurovich, P. I.; Yousufuddin, M.; Bau, R.; Thompson, M. E. *J. Am. Chem. Soc.* **2005**, *127*, 28−29.

(32) (a) Kim, Y.-J.; Han, J.-T.; Kang, S.; Han, W. S.; Lee, S. W. *Dalton Trans.* **2003**, 3357−3364. (b) Johansson, M. H.; Otto, S.; Oskarsson, Å. *Acta Crystallogr.* **2002**, *B58*, 244−250. (c) Connick, W. B.; Marsh, R. E.; Schaefer, W. P.; Gray, H. B. *Inorg. Chem.* **1997**, *36*, 913−922.

(33) Gutmann, V. *The Donor-Acceptor Approach to Molecular Interaction*; Plenum Press: New York, 1978.